Nuclear Physics with OBELIX

The OBELIX Collaboration

A. Ableev[i], A. Adamo[a], A. Andrighetto[l], M. Agnello[b], F. Balestra[g], G. Belli[c],
G. Bendiscioli[d], A. Bertin[e], P. Boccacciof[f], G. Bonazzola[g], T. Bressani[g], M. Bruschi[e],
M.P. Bussa[g], L. Busso[g], D. Calvo[g], M. Capponi[e], P. Cerello[g] , C. Cicalo'[a], M. Corradini[c],
S. Costa[g], S. De Castro[e], F. D'Isep[g], I.V. Falomkin[i], L. Fava[g], A. Feliciello[g], L. Ferrero[g],
V. Filippini[d], T. D. Galli[e], R. Garfagnini[g], U. Gastaldi[f], P. Gianotti[g], A. Grasso[g],
C. Guaraldo[j], F. Iazzi[b], A. Lanaro[j], E. Lodi Rizzini[c], M. Lombardi[f], V. Lucherini[j],
A. Maggiora[g], S. Marcello[g], U. Marconi[e], G.V. Margagliotti[k], G. Maron[f], A. Masoni[a],
I. Massa[e], B. Minetti[b], P. Montagna[d], M. Morando[l], F. Nichitiu[j], D. Panzieri[g], G. Pauli[k],
M. Piccinini[e], G. Piragino[g], M. Poli[m], G.B. Pontecorvo[i], G. Puddu[a], R.A. Ricci[f,l],
E. Rossetto[g], A. Rotondi[d], A.M. Rozhdestvensky[i], P. Salvini[d], L. Santi[n],
M.G. Sapozhnikov[i], N. Semprini Cesari[e], S. Serci[a], P. Spighi[e], P. Temnikov[i], S. Tessaro[k],
F. Tosello[g], V.I. Tretyak[i], G. Usai[a], F. Vannucci[f], S. Vecchi[e], G. Vedovato[f], L. Venturelli[c],
M. Villa[e], A. Vitale[e], A. Zenoni[h], A. Zoccoli[e] and G.Zosi[g]

Presented by M. P. Bussa

[a] Dip. di Scienze Fisiche, Universita' di Cagliari, and INFN - Cagliari, I-09100 Cagliari, Italy
[b] Politecnico di Torino and INFN - Torino, I-10125 Torino, Italy
[c] Dip. di Elettronica per l'Autom. Industriale, Universita' di Brescia, and INFN - Torino,
   I-25060 Brescia, Italy
[d] Dip. di Fisica Nucl. e Teorica, Universita' di Pavia, and INFN - Pavia, I-27100 Pavia, Italy
[e] Dip. di Fisica, Universita' di Bologna, and INFN - Bologna, I-40100 Bologna, Italy
[f] Laboratori Nazionali di Legnaro dell'INFN, I-35100 Padova, Italy
[g] Istituto di Fisica, Universita' di Torino, and INFN - Torino, I-10125 Torino, Italy
[h] Dip. di Elettronica per l'Autom. Industriale, Universita' di Brescia, and INFN - Pavia,
   I-27100 Pavia, Italy
[i] Joint Institute for Nuclear Research, Dubna, SU-101000 Moscow, Russia
[j] Laboratori Nazionali di Frascati dell'INFN, I-00044 Frascati, Italy
[k] Istituto di Fisica, Universita' di Trieste, and INFN - Trieste, I-34127 Trieste, Italy
[l] Dip. di Fisica, Universita' di Padova, and INFN - Padova, I-35100 Padova, Italy
[m] Dip. di Energetica, Universita' di Firenze, and INFN - Bologna, I-40100 Bologna, Italy
[n] Istituto di Fisica, Universita' di Udine, and INFN - Trieste, I-33100 Udine, Italy

Abstract
    Recent experimental results in antinucleon-nucleus interaction obtained by the OBELIX
collaboration at LEAR are presented. Preliminary results concerning the total antineutron-
nucleus annihilation cross section at low energy are reported. They represent the first complete
set of measurements on medium and heavy nuclei available in the momentum region below 300
MeV/c. A new measurement of the exotic one-meson annihilation at rest $\bar{p} d \rightarrow \pi^- p$ (Pontecorvo
reaction) with the better statistics and precision up to now, is reported. Finally, the measurement

of the $K^+K^-/\pi^+\pi^-$ production ratio in $\bar{p}$ annihilation on gaseous D_2 at NTP is presented. From this ratio an upper limit of the P-wave contribution to the $\bar{p}p$ annihilation in GD_2 is inferred.

1. INTRODUCTION

The high performances of the OBELIX apparatus in terms of timing, momentum and angular resolution, together with the capability to measure with great accuracy the final state multiplicities for both charged and neutral particles allowed to develop a nuclear physics program in parallel with the meson spectroscopy program, for which the apparatus was originally designed.

Antineutron-nuclear interaction has so far concerned only one nucleus, in two experiments of the first LEAR era. The OBELIX measurements on five targets, ranging from light to heavy nuclei, give the first set of systematic data in the energy region below 300 MeV/c. The study of the rare reaction $\bar{p}\,d \to \pi^-\,p$, a Pontecorvo reaction, allows to investigate the small distance region or, accordingly, the high momentum components of the target wave function, with the aim to look for an evidence of quark degrees of freedom in nuclear matter. The OBELIX measurement in a dedicated experiment, with data taking specifically designed to select the topology of a Pontecorvo event, with experimental parameters and systematic uncertainties carefully evaluated and, finally, with a sample of good events more than fifteen times greater than the number of events collected by the only counter experiment done up to now,can represent a point of reference for the studies in the field. The determination of the angular momentum states from which the $\overline{N}N$ annihilation at rest occurs is of great importance for the comprehension of the annihilation dynamics. The experimental situation concerning the antiprotonic deuterium is far from being established. For gaseous deuterium, only one measurement is available with a great error. A new determination of the P-wave contribution in the annihilation on gaseous deuterium at NTP has been obtained at the OBELIX spectrometer by measuring with high statistical accuracy the ratio of the K^+K^- to the $\pi^+\pi^-$ annihilations.

2. THE ANTINEUTRON ANNIHILATION ON NUCLEI

2.1. The antineutron facility

The antineutron beam is a facility installed in the OBELIX apparatus [1] , which produces antineutrons via charge-exchange (CEX) in a LH_2 target put upstream the whole apparatus. A sketch of the facility is given in fig. 1. A detailed description of the set-up, together with the operating principles, are given in [2÷4] . The antiprotons of 300 MeV/c delivered by LEAR, after passing a 100 μm Be window, crossed a 80 μm beam scintillator counter, then impinged on the LH_2 Production Target (PT), surrounded by a Veto Box of plastic scintillators. The produced antineutrons were collimated by a long collimator (80 cm lenght, 30 mm diameter), passed through the Reaction Target used in $\bar{n}p$ measurements, obviously empty, and finally impinged on the nuclear targets (NT). A set of five nuclear targets, ranging from light to heavy nuclei (C, Al, Cu, Sn and Pb), was used in the measurement. They consisted of different discs, coaxial to the beam line, 26 cm of diameter and thicknesses inversely proportional to the density, in order to have a nearly constant number of nucleons per cm^2, positioned along the beam line at 36 cm from the center of the apparatus, just behind the reaction target.

The following two subdetectors of OBELIX:
- the Time-Of-Flight (TOF): two coaxial barrels of plastic scintillators (30+90 slabs at 18 cm and 136 cm from the beam axis, respectively; 80 cm and 240 cm long; 1 cm and 4 cm thick, covering an azimuthal angle of 12° and 4°, respectively) for time-of-flight measurements and

charged particle indentification at the trigger level;
  - the Jet Drift Chambers (JDC), from the CERN Axial Field Spectrometer (AFS), for tracking and particle identification by dE/dx measurement. The detector consists of two half cylinders (160 cm diameter, 140 cm length) equipped with 3280 sense wires organized in 82 azimuthal sectors of 4⁰ and three crowns,
allowed to measure, with the technique described in [2,3], for each n̄ -nuclear annihilation:
a) the n̄ momentum; b) the prong multiplicity of the final state; c) the annihilation vertex position.
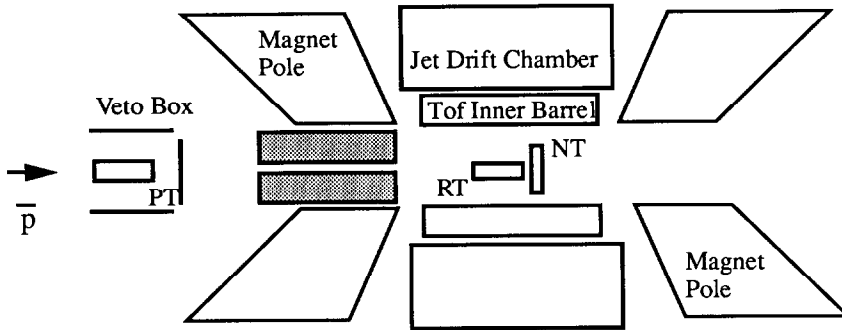
Figure 1. The antineutron facility.

The trigger logic defining the production of an antineutron was given by the antiproton beam counter signal in anticoincidence with the Veto Box signal. An antineutron annihilation event required, to be read out, at least one hit on the TOF scintillator counter inner barrel: the first slab hit after annihilation gave the stop to the time-of-flight measurement, the start being given by the p̄ beam counter signal. The antineutron were produced in the momentum range from CEX threshold (≈ 60 MeV/c) up to about the antiproton momentum. The average n̄ momentum on target was 230 MeV/c. In fig. 2 the distribution of the annihilation vertices, as reconstructed by the JDC drift chambers, is shown. The peak corresponding to the nuclear target is well separated by the background due to the target walls, within the resolution (≤ 1 cm) of the spectrometer in the z direction.

2.2. The antineutron-nucleus annihilation cross section
A sample of 10^3 events was collected for each nuclear target. Multiplicity and quality cuts were applied in order to clean the data sample and improve the accuracy on the vertex position. The efficiency of the quality cuts and of the reconstruction procedure were evaluated on Monte Carlo data with the same procedure used for the n̄-H_2 measurements [4]. Major effects depending on the target finite width, like absorption and energy losses of annihilation products as well as differences in capture on proton and on neutron inside the nucleus were taken into account in the simulation. In fig. 3 the n̄ annihilation cross sections are plotted as a function of $A^{2/3}$. The evaluation of the detector acceptance being still in progress, the data should be scaled by a common normalization factor. The errors quoted include the statistical and normalization uncertainties.

The results are fully consistent with a straight line behavior. For the Pb nucleus the linear fit to the $A^{2/3}$ scaling law overestimates slightly the experimental results. This discrepancy, between the linear behavior predicted by the optical model and the experimental result for Pb nucleus, was also observed in $\bar{p}$ nuclear absorption at higher energies [5].

A fit to the law $\sigma_{ann} = \sigma_0 A^\nu$ gives

$$\nu = 0.65 \pm 0.04 \tag{1}$$

The value of the parameter ν is very close to 2/3, which represents an asymptotic value reached only at much higher momenta, when antiproton nuclear absorption cross sections are considered [6].
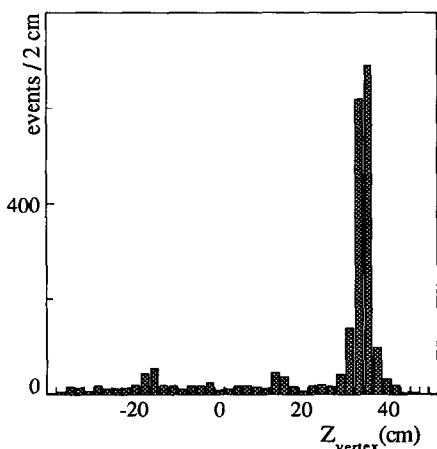
Figure 2. $\bar{n}$ annihilation vertex distribution.
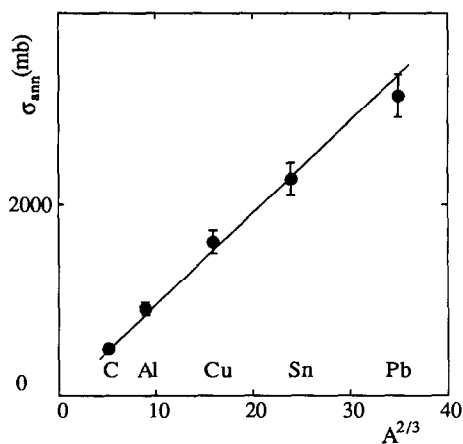
Figure 3. $\bar{n}$ annihilation cross section vs $A^{2/3}$.

As far as the energy dependent parameter $\sigma_0(E)$ is concerned, it includes the global normalization, which is still in progress. Therefore the assumption was made that the agreement between experimental results and extrapolation to A=1 holds for $\bar{n}$ as well as for $\bar{p}$ [7] and the value

$$\sigma_0 = \sigma_{ann}/A^\nu = \sigma_{ann}(H_2) = 170 \text{ mb} \tag{2}$$

was chosen, as calculated from the cross section distribution measured by the same apparatus, taking into account the $\bar{n}$ momentum spectrum. This internal normalization presents many advantages: the same $\bar{n}$ energy spectrum is used to fix an energy dependent parameter; most of the systematic effects coming from the apparatus and the analysis procedure are included in the same way in A=1 and in A>1 measurements.

The antineutron annihilation cross sections after the normalization and the fit results are displayed in fig.4 together with the few existing data, all concerning the $\bar{n}$-Fe annihilation, obtained by other experiments (PS178 and PS199 at LEAR) [8,9]. The comparison with the results of PS178 experiment, which measured σ_{ann} from 100 MeV/c up to 531 MeV/c, in steps

of 40 MeV/c, was obtained by weighting these results with the present experimental momentum distribution. The PS199 result was obtained at 300 MeV/c and is a bit lower than the PS178 one, as predicted by the 1/p behavior of the $\overline{N}N$ reaction cross section. The unique other measurement available, concerning $\overline{n}$-C annihilation at 250 MeV/c [10], is not reported in fig. 4 because affected by large statistical and systematic uncertainties. There is an excellent agreement between the fit to the OBELIX results and the $\overline{n}$-Fe data of PS178 experiment.
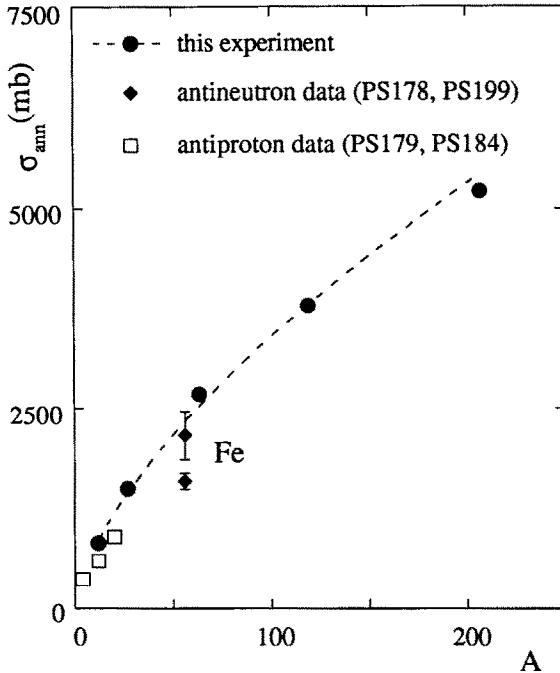
Figure 4. $\overline{n}$ annihilation cross section vs A. For the best fit line and the references, see text.

In fig.4 the $\overline{p}$-A data available in the low energy region [11÷13] are also shown for comparison. All the measurements are limited to light nuclei (A ≤ 20). Where possible (Ne, ^{4}He) a linear interpolation was used to report a value corresponding to the average $\overline{n}$ momentum of 230 MeV/c. The agreement between the $\overline{n}$ and $\overline{p}$ data is good, although the $\overline{p}$-A reaction cross section has a quite irregular dependence on A and on the $\overline{p}$ momentum at low energy and in the light nuclei region [7] .

3. MEASUREMENT OF THE PONTECORVO REACTION $\overline{p}\, d \to \pi^- p$ AT REST

The so-called Pontecorvo reactions [14] constitute a wide class of antinucleon annihilation reactions on nuclei characterized by two-body final states consisting of (not less than) *one baryon* and (not more than) *one meson*.

They include, in particular:
- *Single-meson annihilations*, in which the meson is a *pion*,
- *Mesonless annihilations*, with *two baryons* in the final state:

$$\bar{p} + d \rightarrow \pi^- p \qquad (3)$$

$$\bar{n} + d \rightarrow \pi^+ p \qquad (5)$$

$$\bar{p} + {}^3He \rightarrow n + p \qquad (4)$$

$$\bar{n} + {}^3He \rightarrow p + p \qquad (6)$$

In an ordinary annihilation of an antinucleon on a nucleon on mass-shell, at least two pions must be produced. The process where an antinucleon-nucleon pair is converted into a single meson is forbidden on quasi-free nucleons, because the conservation of momentum and energy cannot be satisfied simultaneously. For that reason, the processes (3÷6), the Pontecorvo reactions, in which only one meson, at most, is the product of the annihilation, are called unusual annihilations. As for other processes in Nuclear Physics, energy-momentum conservation in Pontecorvo reactions can be satisfied by allowing the process to proceed via the collaboration of at least two nucleons. A "multinucleon" annihilation presents indeed strong reasons of interest. Small distance dynamics between nucleons of nuclei, where quark degrees of freedom play an important role, is expected to determine the amplitude of reactions.

Despite the motivations, the Pontecorvo reactions have not yet been experimentally measured, with the only exception of the reaction (3), for which two only published data at rest exist, both statistically scarce. They rely upon 6 measured events in bubble chamber [15], with a branching ratio

$$B.R. \, (\bar{p} d \rightarrow \pi^- p) = N(\bar{p} d \rightarrow \pi^- p) / N(\bar{p} d \rightarrow all) = (0.9 \pm 0.4) \, 10^{-5} \qquad (7)$$

and on 5 events measured by ASTERIX collaboration at LEAR [16], with a branching ratio

$$B.R. \, (\bar{p} d \rightarrow \pi^- p) = (1.4 \pm 0.7) \, 10^{-5} \qquad (8)$$

For this reason, a new measurement of antiproton absorption in deuterium, with the better precision and statistics up to now, was performed using the OBELIX spectrometer at LEAR.

3.1. Data taking and trigger configuration

The antiprotons of 105 MeV/c supplied by LEAR were stopped in a cylindrical (ø: 30 cm) gaseous target filled by deuterium at NTP. The stop distribution was spread, around the center of the target, along the beam axis by $\sigma_z = 5$ cm, the transverse spread being $\sigma_x = \sigma_y = 2$ cm. The contamination from annihilations on the target walls (50 mm thick) was negligible; the annihilations in flight were some part per thousand of the total number of annihilations.

The trigger was designed to select the topology of an event characterized by two correlated back-to-back long tracks belonging to high momentum charged particles. The background contaminating the signal was constituted mainly by reactions with a neutron spectator $\bar{p} d \rightarrow \pi^+\pi^- n_s$ and $\bar{p} d \rightarrow K^+K^- n_s$. The data were collected under two different trigger configurations:

- *HARD trigger*. It required the coincidence of the beam counter signal with a highly selective back-to-back correlation in the TOF barrels. Specifically, it was requested: only two hits in the inner barrel, on two opposite slabs chosen among three adjacent; only two hits in the outer barrel, on two opposite slabs chosen among two adjacent ($\pm 8°$ in azimuthal angle). The external slabs were fixed in the measurement, thus selecting the back-to-back trigger configuration,

- *SOFT trigger*. It was characterized by a looser request on the outer barrel: two hits on two opposite slabs chosen among three adjacent (±12° in azimuthal angle)

Moreover, a significant difference between the two configurations was represented by the experimental lay-out adopted in the two cases. In data taking with the HARD trigger, the SPC chamber, with its internal target, was removed and replaced by a large deuterium target of 30 cm diameter, 75 cm length and an entrance mylar window of the same thickness. Therefore, in this set-up annihilations on the target walls were negligible. An overall number of about $6 \cdot 10^4$ events using the SOFT trigger and of about $7 \cdot 10^4$ events using the HARD trigger were collected. Moreover, a sample of about 10^4 minimum bias events, characterized by the unique requirement of having an antiproton hitting the beam counter scintillator, was also collected.

3.2. Data analysis and results

The events were reconstructed by the OBELIX reconstruction program. The program was required to perform a vertex fit in the target region; if the fit failed, due to the high degree of collinearity of the tracks, track parameters were extrapolated with errors up to the minimum approach point to the beam axis.

Only events with two tracks of opposite sign were accepted. A filter on the track quality was applied by restricting the solid angle in the jet chambers to a fiducial volume containing only long tracks. The acceptance and the efficiency of the quality cut was evaluated by comparing Monte Carlo and real data for the $\bar{p}\, d \to \pi^+\pi^-\, n_S$ reaction, assumed as reference reaction thanks to the geometrical collinearity and to the high momentum of the tracks.
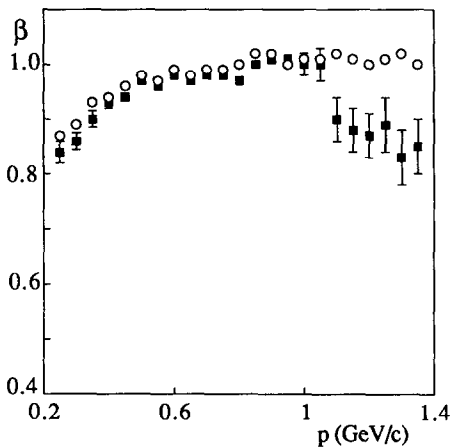
Figure 5. β vs p for positive (full squares) and negative (open circles) particles.
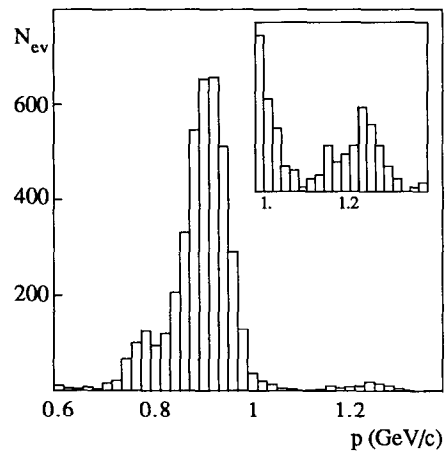
Figure 6. Momentum distribution for collinear events.

Fig.5 shows the β distribution as a function of the momentum both for positive and for negative particles. The proton contribution is dominant in the momentum region above 1 GeV/c.

The momentum distribution for collinear events (relative angle $\geq$ 175°) in Fig.6 shows the peaks of the background channels $\pi^+\pi^-\, n_S$ and $K^+K^-\, n_S$. A signal from the Pontecorvo reaction at 1.25 GeV/c is visible.

A first filter was used to select events containing a proton through a 3 σ cut on the time of

flight of positive particles. The data sample was then submitted to the kinematical fit to eliminate any contamination from the $\pi^+\pi^-$ n_s and K^+K^- n_s reactions. A cut at the confidence level of 0.1% (events with $\chi < 10$) was applied.
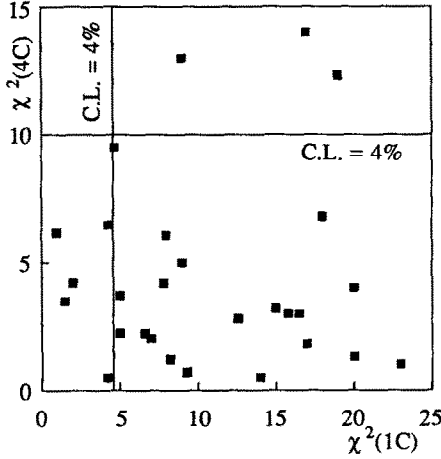
Figure 7. $4C\chi^2$ distribution of events for the π^- p hypothesis vs $1C\chi^2$ distribution for the $\pi^-\pi^0$ p hypothesis.

No one of the rejected events fitted the p π^- hypothesis better than the contamination channels considered. The attribution to the channel $\bar{p}$ d $\rightarrow$ π^- p and the separation from the possible contaminating reaction $\bar{p}$ d $\rightarrow$ π^- π^0 p was made on the basis of the kinematical fit (fig.7). At 4% confidence level 54 and 23 events out of the two data samples obtained, respectively, with the HARD and the SOFT trigger configurations, were attributed to the Pontecorvo channel. 4 and 3, respectively, of them were compatible with both hypotheses, but were attributed to the Pontecorvo channel on the basis of relative probability of the fit. A systematic error corresponding to 7 and 3, respectively, not attributed events should be considered. They are due to the difficult calibration of the global system in such high momentum region, that influences the kinematical fit selectivity.

The absolute branching ratio for $\bar{p}$ d $\rightarrow$ π^- p is defined as

$$\text{B.R.} = \frac{N(\bar{p}\,d \rightarrow \pi^-\,p)}{N(\bar{p}\,d \rightarrow \text{all})} = \frac{N_{ev}\frac{1}{\varepsilon}}{N^d_{ann}(1 + \varepsilon_n)(1 + \varepsilon_m)} \tag{9}$$

where: $N(\bar{p}\,d \rightarrow \pi^-\,p)$ is the number of Pontecorvo events
$N(\bar{p}\,d \rightarrow \text{all})$ is the total number of annihilations in deuterium
N_{ev} is the number of measured Pontecorvo events
N^d_{ann} is the number of detected annihilations
ε is the product of the various efficiencies = $\varepsilon_t\cdot\varepsilon_g\cdot\varepsilon_v\cdot\varepsilon_q\cdot\varepsilon_r\cdot\varepsilon_c$
ε_n is the loss factor due to unseen "zero-prong" events
ε_m is the contamination factor due to the target mylar walls.

Table 1 summarizes the relevant experimental parameters of the measurement for deducing the Pontecorvo branching ratio.

Table 1
B.R.($\bar{p}$ d $\rightarrow$ π^- p at rest) - experimental parameters

	HARD trigger	SOFT trigger
Data sample	$7 \cdot 10^4$	$6 \cdot 10^4$
N^d_{ann} number of detected annihilations	$9.94 \cdot 10^8$	$3.66 \cdot 10^8$
N_{ev} number of Pontecorvo events	54	23
ε_n "zero prong" loss factor	0.018	0.018
ε_m target wall contamination	-	0.04
ε_t trigger efficiency	0.91	0.87
ε_g geometrical trigger acceptance	0.008	0.0119
ε_v fiducial volume acceptance	0.90	0.82
ε_q quality cut efficiency	0.76	0.72
ε_r reconstruction efficiency	0.94	0.89
ε_c kin. fit confidence level	0.96	0.96

From (9) and Table 1, one gets the values reported in Table 2.

Table 2
B.R. of the Pontecorvo reaction for the two OBELIX data samples

	HARD trigger	SOFT trigger
B.R. ($\bar{p}$ d $\rightarrow$ π^- p)	$(1.19 \pm 0.16) \cdot 10^5$	$(1.23 \pm 0.26) \cdot 10^5$

By properly combining [17] the branching ratios obtained with the HARD trigger and with the SOFT trigger, one gets:

$$\text{B.R. } (\bar{p} d \rightarrow \pi^- p) = (1.20 \pm 0.14) \cdot 10^5 \tag{10}$$

A certain number of systematic effects have been studied. For some of them, which affected the total number of annihilations in the target, value and sign of the correction were identified and thus it was possible to include them in calculating the branching ratio (see ε_n and ε_m). The most important of other systematic effects affected mainly the:

- *trigger efficiency*: in evaluating the efficiency of the group of slabs of the TOF barrels participating to the trigger, a systematic component of uncertainty, coming from the single slab fluctuations around the average number of hits and from the normalization criteria adopted, could be estimated to be of the order of 5%;

- *reconstruction efficiency*: a systematic uncertainty on the reconstruction efficiency could be evaluated to be of the order of 1.5%;

- *kinematical fit selectivity*: a systematic error coming from the calibration of the whole detector had to be taken into account. Considering the number of events which could not be assigned, this global systematic uncertainty was evaluated to be around 13% both for the HARD and for the SOFT trigger configuration.

The contamination from cosmic ray events was excluded, by checking that the slabs fired in each event had a time sequence proper of a two-prong event coming from the target.

Due to the above systematic effects, the absolute branching ratio of the Pontecorvo reaction must be corrected by a factor

$$f_{syst} = (1.00 \pm 0.19) \tag{11}$$

4. ANGULAR MOMENTUM STATES IN $\bar{p}$ d ANNIHILATION AT REST

The determination of the angular momentum states from which the $\overline{N}N$ annihilation at rest occurs is of great importance for the comprehension of the annihilation dynamics [18]. Following the model of [19], the annihilation fraction in S and P waves from protonium and antiprotonic deuterium at rest can be deduced from the ratio of the branching ratios ($K^+K^-/\pi^+\pi^-$) into two charged mesons and kaons. In general, a precise measurement of this ratio is a test for any model dealing with the initial state of the antiprotonic atoms.

The experimental situation concerning the antiprotonic deuterium is far from being established. Data are scarce in the gaseous deuterium, for which only one measurement [20] is available with large error. On the side of the liquid deuterium the measurements, obtained with different techniques and at different level of statistical significance, are quite controversial [21]. The interest for the antiprotonic deuterium comes also from the apparent breakdown of the charge invariance in antiproton annihilation on proton and neutron, that could suggest a resonant $\overline{N}N$ behavior at threshold [19] . In this framework, the presence of effects on the spectator momentum would give indication of energy sensitive $\overline{N}N$ phenomena.

4.1. New measurement of $K^+K^-/\pi^+\pi^-$ ratio from $\bar{p}$ d annihilation at rest

A new determination of the relative S and P wave contributions in gaseous D_2 at NTP has been obtained at the OBELIX spectrometer by measuring with high statistical accuracy the ratio R of the K^+K^- to the $\pi^+\pi^-$ annihilations [22]. The reliability of the analysis procedure, described below, was checked by remeasuring the ratio R for gaseous H_2 at NTP. The H_2 events were collected under the same trigger conditions of D_2 in the same period of data taking.

The value obtained for R in gaseous H_2 at NTP is

$$R_{GH} = 0.163 \pm 0.011 \tag{12}$$

in good agreement with the value $R_{GH} = 0.161 \pm 0.009$ reported by Doser et al [38].

The analysis procedure of the D_2 data took advantage of the quasi two-body nature of the reactions under study, i.e. the average momentum and the average β for the pair of particles of opposite charge was considered. This leads to an improvement of the momentum and β

resolution by a factor $\sqrt{2}$ with respect to the single track resolution (60 MeV/c FWHM and 20% FWHM, respectively).

Loose collinearity criteria $(\Delta\theta<25^\circ, \Delta\phi<25^\circ)$ were used to select the events, in order to avoid tight cuts on the neutron spectator momentum, which might bias the interpretation of the data. The events were furthermore submitted to the 1C kinematical fit to the K^+K^- n_s and $\pi^+\pi^-$ n_s hypotheses, n_s being the neutron spectator. Only the events passing the fit with a CL>10% were accepted for further analysis. The average momentum distribution of the two tracks for the events fitting the kinematical hypotheses are shown in fig.8a. A clean separation between the K^+K^- n_s and $\pi^+\pi^-$ n_s events is evident even if some residual background from the contaminating reactions is expected. The background comes mostly from the $\pi^+\pi^-\pi^0 n_s$ channel: the resulting Monte Carlo distribution for events satisfying the trigger requirements and selection criteria described above exhibits a peak close to the position of the true K^+K^- n_s events. On the other end, the contamination does not reach the $\pi^+\pi^-$ n_s peak.

The particle identification by means of the time-of-flight was used to reject the residual contamination from pions under the K^+K^- peak. The cut on $<\beta>$ to be applied was tuned before on Monte Carlo events: with a cut on $<\beta>$ >0.98 no K^+K^- events survived, while the efficiency for $\pi^+\pi^-$ events is $(50\pm1)\%$. The background from pions identified by $<\beta>$ cut and corrected for the cut efficiency are shown in fig. 8a. Finally, corrections for different trigger acceptances, arising mainly from the different curvature of pion and kaon tracks, were applied. The systematic effects contribution was supposed to cancel out in the ratio. The value obtained

$$R_{GD} = 0.27 \pm 0.02 \tag{13}$$

is consistent with the previous result of R = 0.36 ± 0.08 [20] , within the statistical error.

The ASTERIX collaboration at LEAR has obtained the partial widths $\gamma_L = \Gamma_L/\Gamma$ for the the $\bar{p}p$ annihilation into K^+K^- and $\pi^+\pi^-$ for initial S and P states separately [20]. With the help of these partial widths, following [19], the fraction of P-wave annihilation

$$P_{GD}=(18 \pm 7)\% \tag{14}$$

in gaseous D_2 at NTP is derived. This result is consistent with the only existing result obtained [37], with a large error, using the ASTERIX data: $P_{GD}=(-5 \pm 20)\%$.

The disagreement observed could be explained in terms of different cuts applied to the n_s momentum [19,23]. Due to the Fermi motion of the nucleons, the $\bar{p} N$ angular momentum can be different from the angular momentum of the $\bar{p}$-deuteron system. As a consequence, S and P-wave annihilations can be reached from both S and P atomic orbitals. Whereas the distribution of the n_s momentum has a classic Hulten shape for annihilations in S-wave or coming from P orbitals, the P-wave annihilations from S-orbital give rise to a characteristic high momentum tail.

Cuts on the spectator momentum can therefore reduce this contribution to a very small level. Following these observations, a refined study of the spectator momentum distribution for both channels K^+K^- n_s and $\pi^+\pi^-$ n_s was performed.

Monte Carlo events were generated for both channels and for different percentages of S and P-wave. The simulated events were subject to the same trigger requirements and analysis filters as the real data. In fig. 8b the experimental n_s momentum distributions for the real $\pi^+\pi^-$ n_s events and for Monte Carlo events generated within the $P_{GD}= 20\%$ hypothesis are compared.

The agreement obtained confirms indirectly the results obtained previously by a completely different method.

As far as the K^+K^- n_s events are concerned, the experimental n_s momentum distribution obtained after the filter of the kinematical fit looks richer in high momentum region in comparison with the $\pi^+\pi^-$ n_s events (fig.8c). However, when the contamination from pions is

rejected by means of the TOF particle identification, the high momentum tail disappears and the K^+K^- n_s distribution looks like the $\pi^+\pi^-$ n_s one. The resulting K^+K^- n_s distribution is presented in fig.8d together with Monte Carlo results for the $P_{GD}= 20\%$ hypothesis.
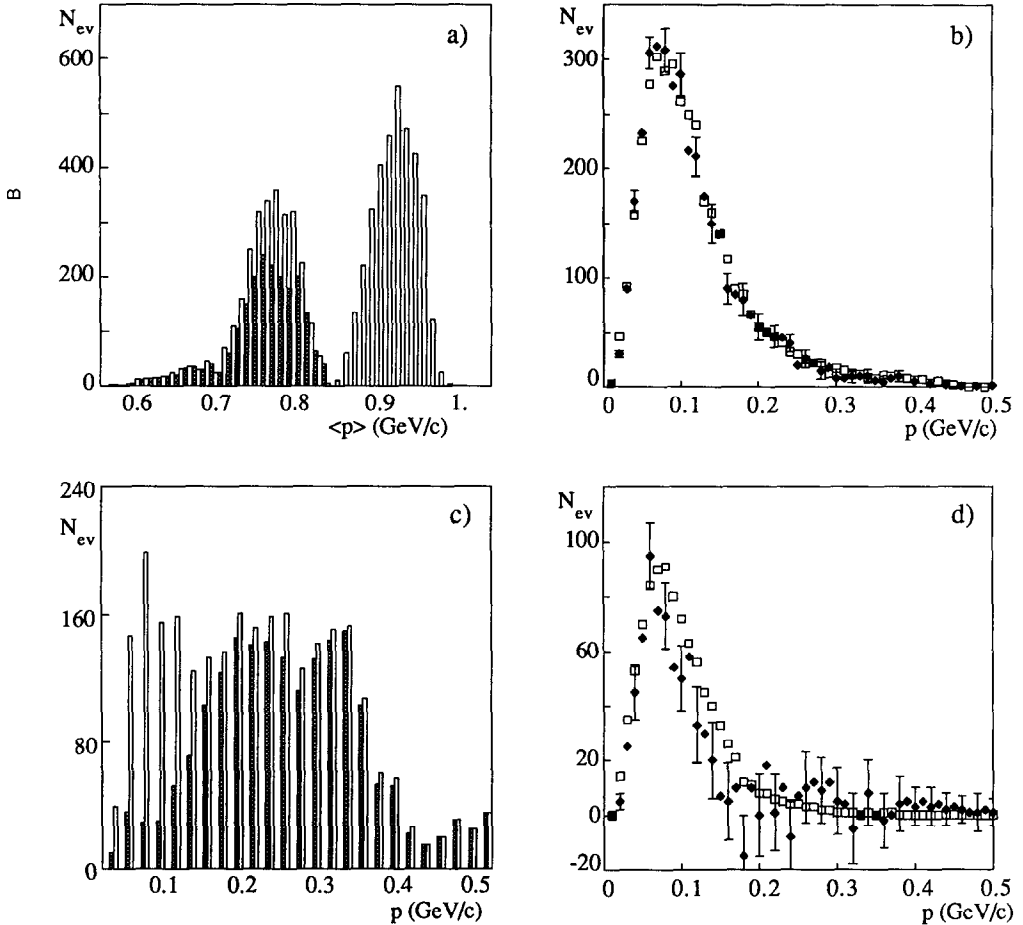
Figure 8. (a) Average momentum of the two tracks after the collinearity cut and kinematical fit selection for K^+K^- n_s and $\pi^+\pi^-n_s$ hypotheses; $\pi^+\pi^-\pi^0 n_s$ background within the K^+K^- n_s events as obtained by particle identification with time-of-flight (hatched histogram). (b) Spectator neutron momentum distribution for $\pi^+\pi^-$ n_s events; Monte Carlo events relative to the 20% P-wave 80% S-wave hypothesis (open squares). (c) Spectator neutron momentum distribution for K^+K^- n_s events; $\pi^+\pi^-\pi^0 n_s$ background as obtained by particle identification with time-of-flight (hatched histogram). (d) Spectator neutron momentum distribution for K^+K^- n_s events after the background subtraction; Monte Carlo events relative to the 20% P-wave 80% S-wave hypothesis (open squares).

In conclusion the OBELIX result weakens somewhat the hypothesis of ref.19, according to which cuts on spectator momentum reduce P-wave annihilation. In fact, loose collinearity cuts were applied accepting also high momentum spectators, but the high momentum tail resulted to be produced mostly by events with misidentified pions. The scarce contribution of the P-wave to the $\bar{p}$ GD_2 annihilation in respect to the $\bar{p}$ GH_2 one remains an open problem.

5. REFERENCES

1 A. Adamo et al., Sov. J. Nucl. Phys. 55 (11) (1992) 1732.
2 F. Iazzi, Proc. 1º Workshop on Intense Hadron Facilities and Antiproton Physics, T. Bressani et al. eds., SIF, Bologna 1990, p. 171.
3 M. Agnello et al., Conf. record of the 1991 IEEE Science Symp. and Medical Imaging, Santa Fe' 1991, vol. 1, p. 404.
4 F. Iazzi, this Conference.
5 V.Ashford et al., Phys. Rev. C31 (1985) 663.
6 J.Vandermeulen, Phys. Rev.Comm. C33 (1986) 1101.
7 G. Bendiscioli, A Review of Antinucleon-Nucleon and Antinucleon-Nucleus Data, Pavia University Report FNT/BE- 91/34 (1991) and references quoted therein.
8 M. Agnello et al., Europh. Lett. 7 (1988) 13.
9 R. Birsa et al., Proc. First Biennal Conference on Low Energy Antiproton Physics (LEAP), Stockholm 1990, p.211.
10 B. Gunderson et al., Phys. Rev. D23 (1981) 587.
11 F. Balestra et al., Nuovo Cimento A100 (1988) 323.
12 D. Garreta et al., Phys. Lett. 149B (1984) 64.
13 F. Balestra et al., Nucl. Phys. A452 (1986) 573.
14 B. M. Pontecorvo, Zh. Exsp. Teor. Fiz. 30(1956) 947.
15 R. Bizzarri et al., Lett. Nuovo Cimento 2 (1969) 431.
16 J. Riedlberger et al., Phys. Rev. C40 (1989) 2717.
17 Review of Particle Properties, Phys. Rev. D45 (1992) I.7.
18 R. Bizzarri et al., Nucl. Phys. B69 (1974) 307.
19 G. Reifenröther and E. Klempt, Phys. Lett. B245 (1990) 129.
20 M. Doser et al., Nucl. Phys. A486 (1988) 493.
21 A. Angelopoulos et al., Phys. Lett., B212 (1988) 129.
22 A. Adamo et al., Phys. Lett. B284 (1992) 448.
23 R. Bizzarri et al., Nucl. Phys. B69 (1974) 298.